Electronic Supplementary Information (ESI)†

Cocrystallization of multi-kinase inhibitor pazopanib with fenamic acids: Improving dissolution and inhibiting cell migration

Sunil K. Rai,*[ac] Anilkumar Gunnam,[b] Debopriya Roy,[de] Raveena Rajput,[d] Kiran Kulkarni[de] and Ashwini K. Nangia*[bc]

[a.] Department of Chemistry, Faculty of Science, University of Lucknow, Lucknow, Uttar Pradesh 226007, India

[b.] School of Chemistry, University of Hyderabad, Prof. C. R. Rao Road, Gachibowli, Central University P.O., Hyderabad 500 046, India

[c.] Division of Organic Chemistry, CSIR − National Chemical Laboratory, Dr. Homi Bhabha Road, Pune 411008, India

[d.] Biochemical Sciences Division, CSIR-National Chemical Laboratory, Dr. Homi Bhabha Road, Pune-411008

[e.] Academy of Scientific and Innovative Research (AcSIR), New Delhi-110025, India

Email: sunilbhu28@gmail.com, ashwini.nangia@gmail.com

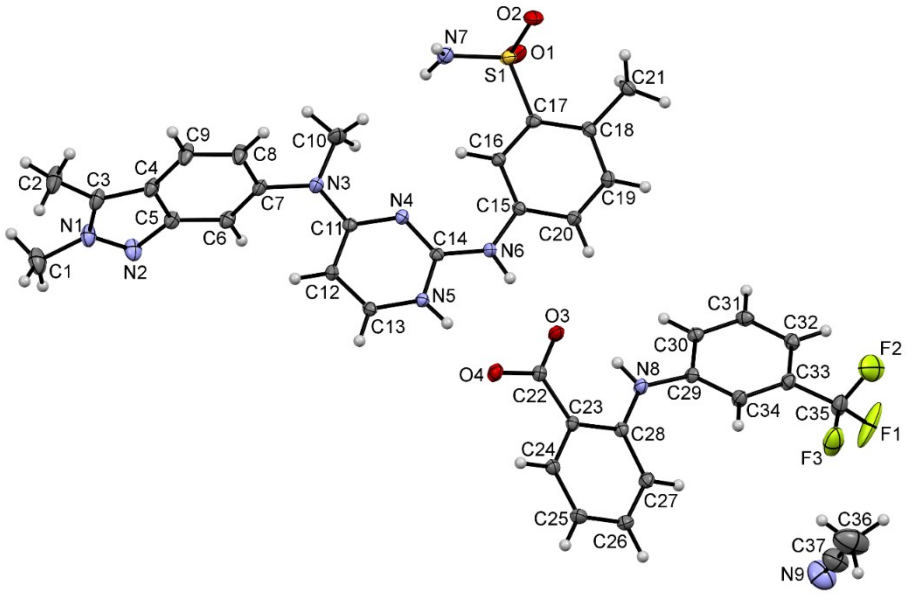

Fig. S1. ORTEP diagram of $PAZ^{+}\cdot FFA^{-}\cdot ACN$ form I. Thermal ellipsoids are drawn at 50% probability level.

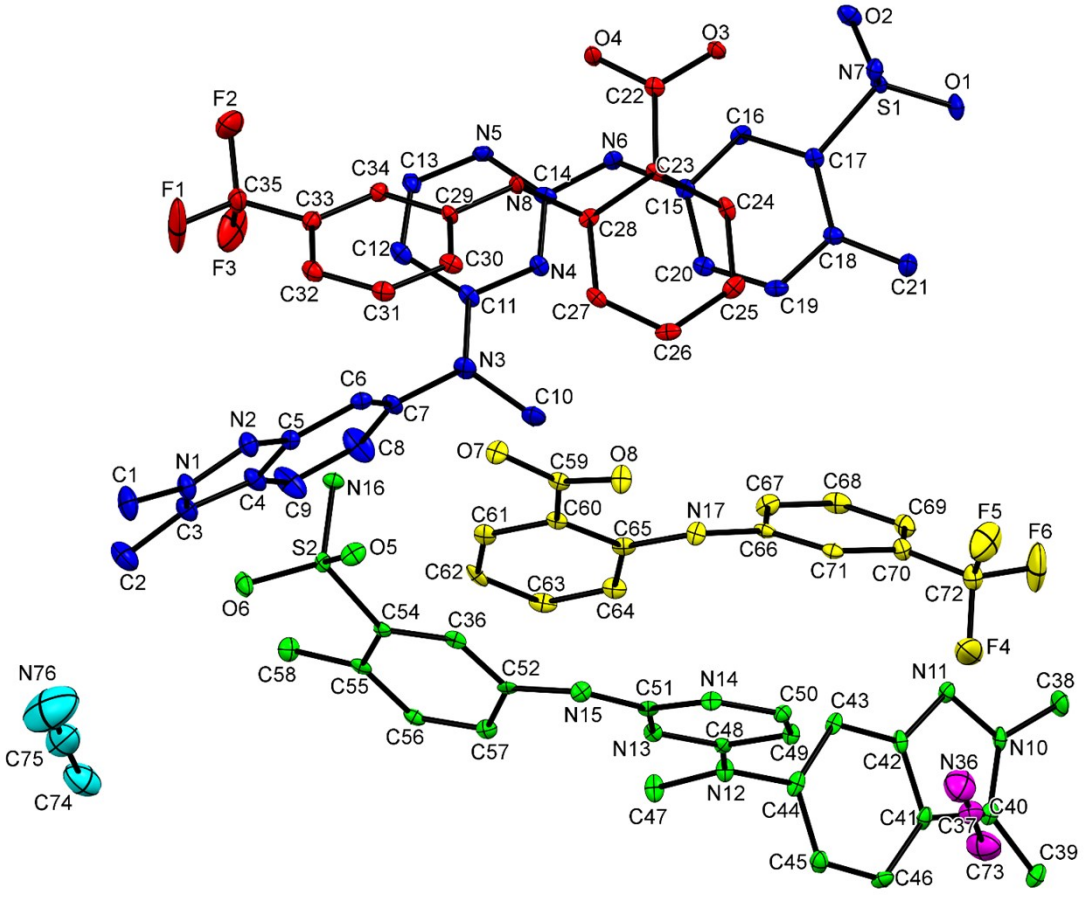

Fig. S2. ORTEP diagram of $PAZ^{+}\cdot FFA^{-}\cdot ACN$ form II. Thermal ellipsoids are drawn at 50% probability level. Hydrogen atoms are omitted for clarity of the picture and molecular colors are shown by symmetry equivalence.

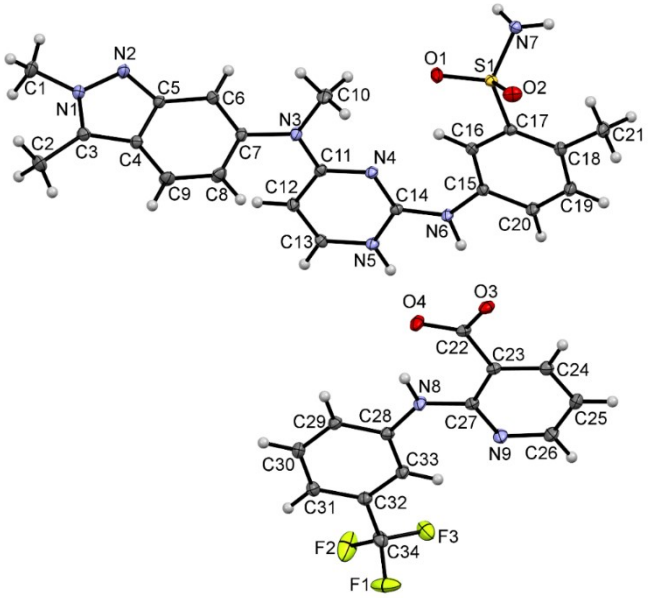

Fig. S3. ORTEP diagram of $PAZ^{+}\cdot NFA^{-}$. Thermal ellipsoids are drawn at 50% probability level.

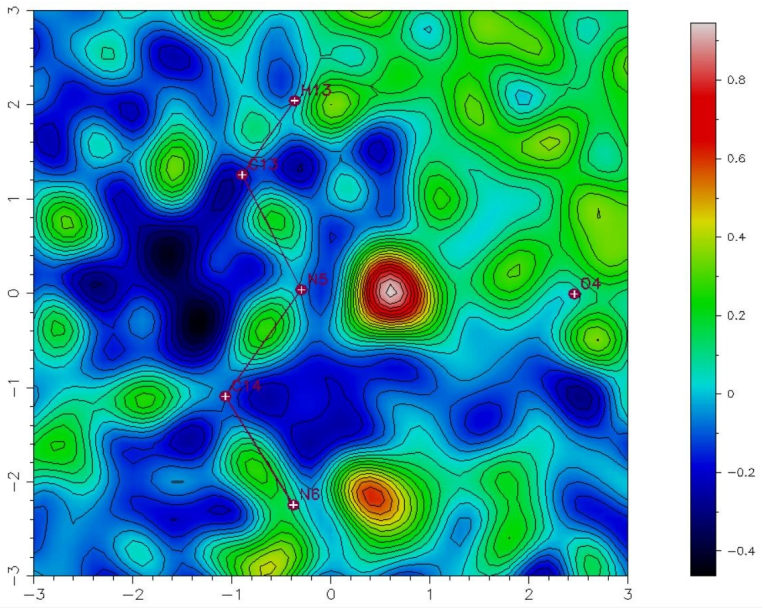

Fig. S4. Fourier difference maps for $PAZ^{+}\cdot FFA^{-}\cdot ACN$ form I showing the electron density in heterodimer '2-aminopyrimidine and –COOH' with the hydrogen atoms in the linking hydrogen bonds omitted from the models. For atom numbering see ORTEP diagram.

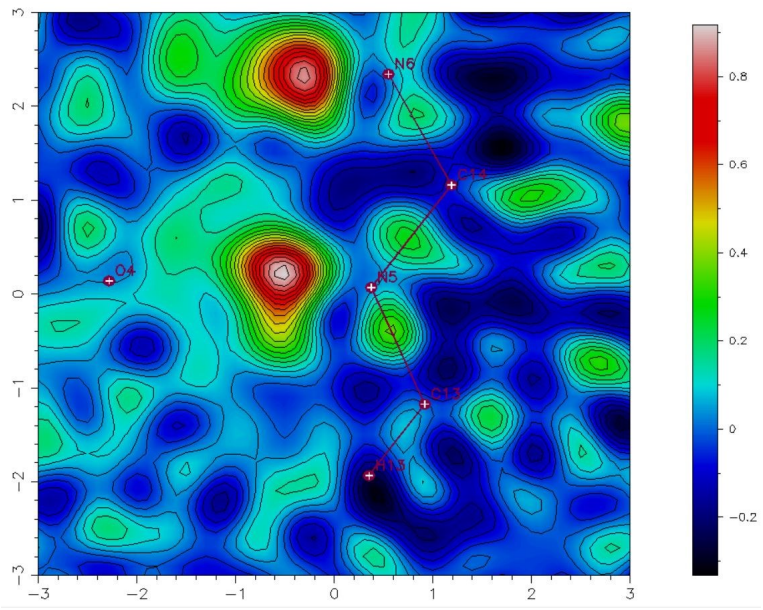

Fig. S5. Fourier difference maps for $PAZ^{+}\cdot NFA^{-}$ showing the electron density in heterodimer '2-aminopyrimidine and –COOH' with the hydrogen atoms in the linking hydrogen bonds omitted from the models. For atom numbering see ORTEP diagram.

Table S1. Geometrical Parameters of Potential Intra- and Intermolecular Interactions in $PAZ^{+}\bullet FFA^{-}\bullet ACN$ form I and II and $PAZ^{+}\bullet NFA^{-}$.

D–H···A	H···A (Å)	D···A (Å)	D–H···A (deg)	symmetry code
		$PAZ^{+}\bullet FFA^{-}\bullet ACN$ (I)		
N5–H5···O4	1.92	2.7601(1)	175	1-x,-y,1-z
N6–H6···O3	1.85	2.7373(1)	175	1-x,-y,1-z
N7–H7A···N9	2.16	2.9938(1)	163	1-x,1-y,-z
N7–H7B···O4	1.97	2.8457(1)	173	x,1+y,z
N8–H8A···O3	1.82	2.5967(1)	149	Intra
C13–H13···O2	2.48	3.0338(1)	117	-1+x,y,z
C16–H16···N4	2.36	2.9546(1)	121	Intra
C16–H16···N7	2.57	3.0054(1)	108	Intra
C20–H20···O3	2.45	3.2178(1)	138	1-x,-y,1-z
C21–H21C···O2	2.51	3.0762(1)	117	Intra
C24–H24···O4	2.43	2.7648(1)	101	Intra
		$PAZ^{+}\bullet FFA^{-}\bullet ACN$ (II)		
N5–H5···O3	1.82	2.674(3)	176	2-x,1-y,1-z
N6–H6···O4	1.93	2.771(3)	167	2-x,1-y,1-z
N7–H7A···N11	2.39	3.130(3)	158	1+x,y,z
N7–H7B···O3	1.83	2.847(3)	168	x,y,z
N8–H8A···O4	2.07	2.676(3)	127	Intra
N14–H14···O7	1.64	2.684(3)	173	1-x,1-y,-z

N15–H15···O8	1.96	2.795(3)	165	1-x,1-y,-z
N16–H16A···O7	1.91	2.901(3)	169	x,y,z
N16–H16B···N2	2.24	3.039(3)	171	x,y,z
N17–H17···O8	2.06	2.690(3)	130	Intra
C1–H1C···O1	2.47	3.226(4)	136	x,-1+y,z
C10–H10C···N4	2.29	2.741(3)	108	Intra
C16–H16···O2	2.38	2.826(3)	108	Intra
C20–H20···N4	2.37	2.879(3)	115	Intra
C21–H21A···O1	2.53	2.950(3)	107	Intra
C24–H24···O3	2.45	2.784(3)	101	Intra
C34–H34···O2	2.50	3.411(4)	168	2-x,1-y,1-z
C36–H36···O5	2.40	2.813(3)	107	Intra
C38–H38B···O6	2.44	3.359(4)	160	-1+x,1+y,z
C39–H39C···F5	2.52	3.286(4)	137	-x,2-y,-z
C47–H47A···N13	2.27	2.728(3)	108	Intra
C57–H57···N13	2.40	2.907(3)	114	Intra
C58–H58A···O6	2.40	2.999(3)	121	Intra
C61–H61···O7	2.45	2.780(3)	101	Intra
C71–H71···O5	2.41	3.299(4)	160	1-x,1-y,-z
C74–H74C···O1	2.48	3.356(4)	152	2-x,1-y,1-z
		PAZ^{+}•NFA^{-}		
N5–H3···O4	1.75	2.6589(1)	173	-x,1/2+y,1/2-z
N6–H4···O3	1.83	2.7578(1)	172	-x,1/2+y,1/2-z
N7–H5A···N2	2.10	2.9399(1)	163	1-x,-1/2+y,1/2-z
N7–H5B···O3	1.98	2.8646(1)	172	1-x,1/2+y,1/2-z
N8–H7···O4	1.85	2.6423(1)	144	Intra
C1–H1C···O1	2.58	3.4797(2)	153	1-x,1-y,1-z
C13–H13···O2	2.37	3.3183(2)	178	-x,1/2+y,1/2-z
C16–H16···O1	2.40	2.8261(1)	107	Intra
C16–H16···N4	2.31	2.9182(1)	121	Intra
C20–H20···O3	2.56	3.2786(1)	132	-x,1/2+y,1/2-z
C21–H21A···O2	2.28	2.9854(1)	128	Intra
C21–H21C···F3	2.46	3.2506(1)	138	-1+x,1/2-y,-1/2+z
C29–H29···O2	2.59	3.4396(2)	149	x,y,z
C33–H33···N9	2.34	2.9417(1)	120	Intra

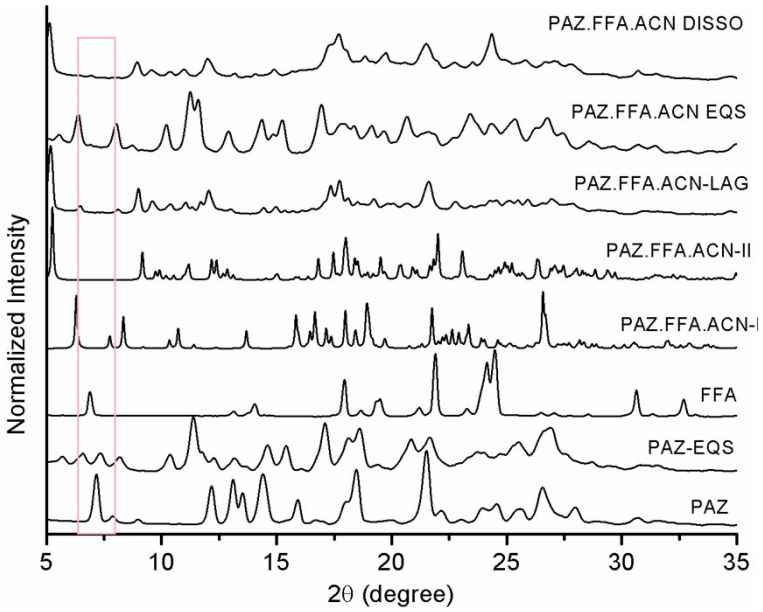

Fig. S6. PXRD pattern overlay of pazopanib (PAZ), residual solid of PAZ in pH 1.2 equilibrium solubility medium (PAZ-EQS), flufenamic acid (FFA), PAZ·FFA·ACN-I, PAZ·FFA·ACN-II and acetonitrile drop grinding preparation of PAZ·FFA·ACN-II (PAZ·FFA·ACN-LAG), residual solid in pH 1.2 equilibrium solubility medium of PAZ·FFA·ACN-II (PAZ·FFA·ACN-EQS), and undissolved solid of PAZ·FFA·ACN-II after dissolution experiment under pH 1.2 dissolution medium.

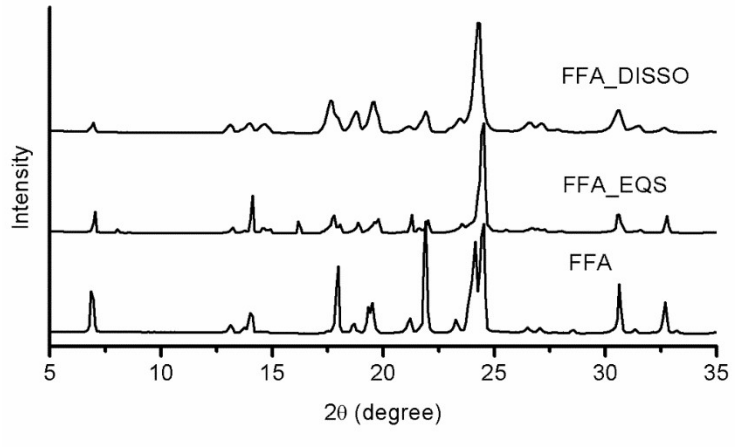

Fig. S7. PXRD pattern overlay of FFA, residue in the pH 1.2 equilibrium solubility medium, and left over solid after dissolution experiment under pH 1.2 dissolution medium.

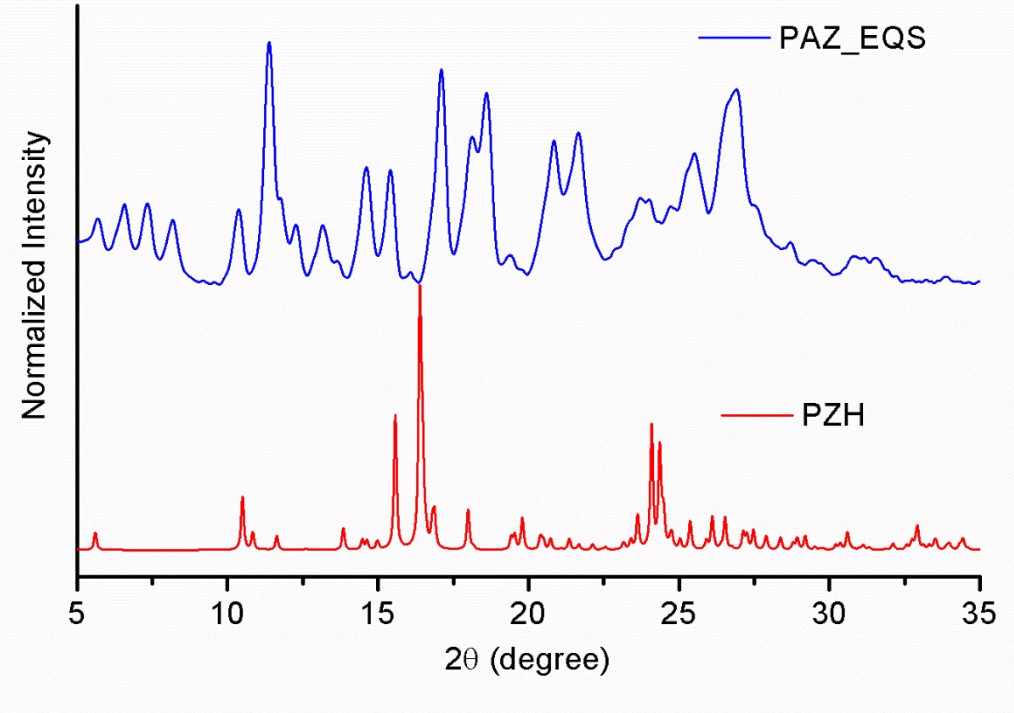

Fig. S8. PXRD pattern overlay of pazopanib hydrochloride (PZH) and, residue PAZ in the pH 1.2 equilibrium solubility medium. PXRD pattern of PZH was taken from published data in *Powder Diffr.*, **2021**, 36, 205-207.

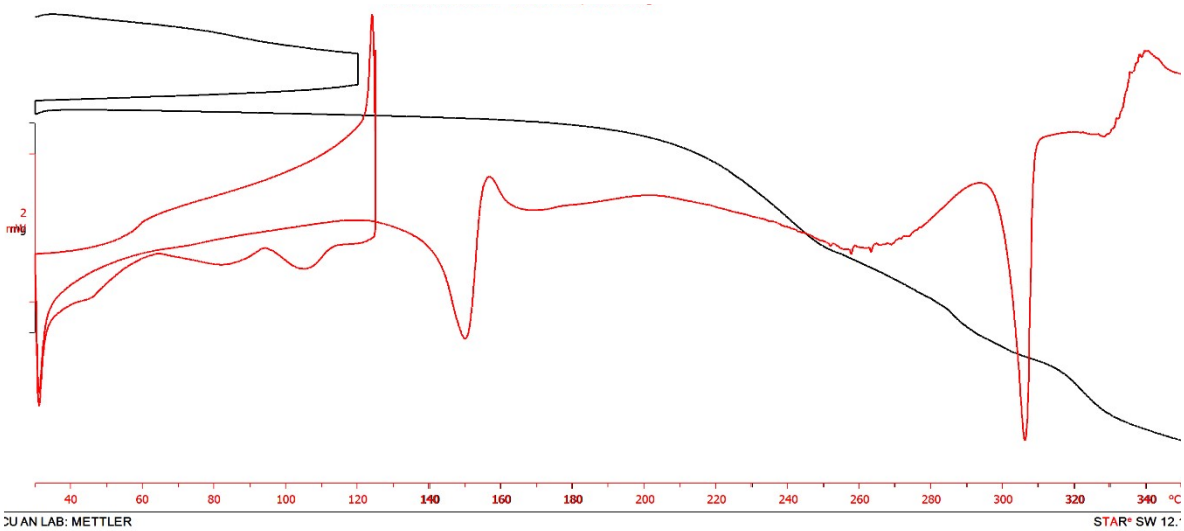

Fig. S9. DSC (red line) and TGA (black line) overlay of $PAZ^{+}\cdot FFA^{-}\cdot ACN$ for heat-cool cycles. First heating cycle 30-120°C with heating rate 10°C/min with an isotherm at 120 °C for 15 minutes followed by cooling to 30 °C with heating rate 10°C/min. After an isotherm at 30°C for 15 minutes a second heating cycle 30-350°C with heating rate 10°C/min was performed.

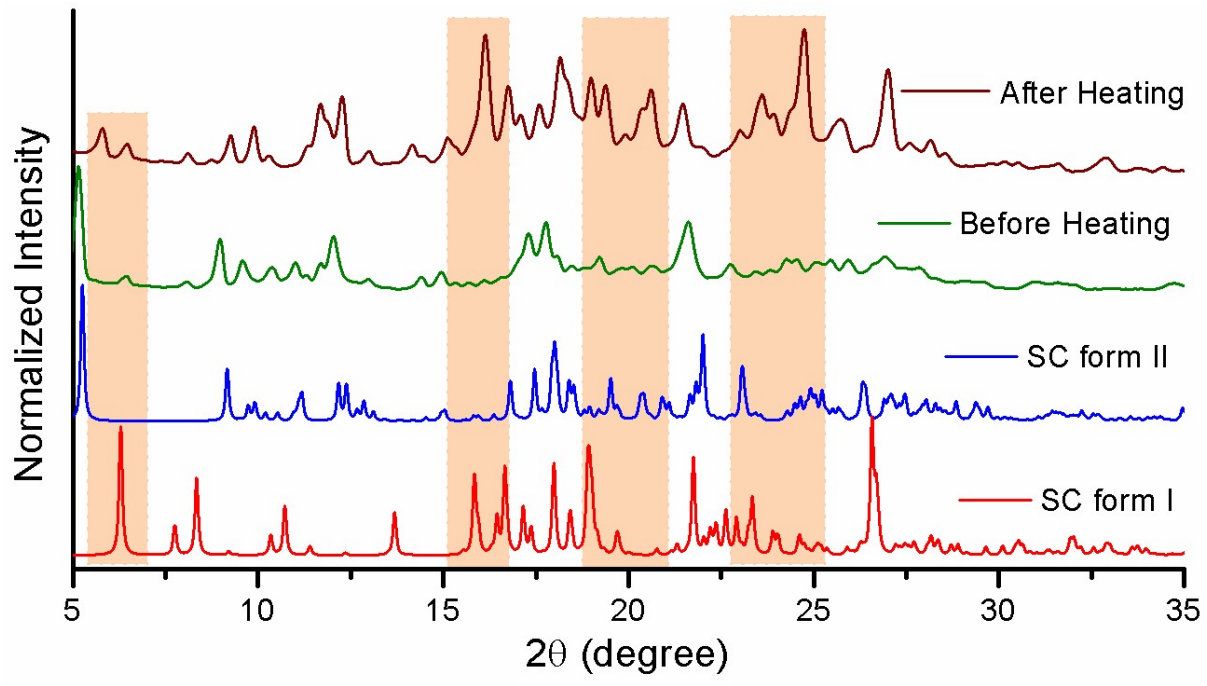

Fig. S10. PXRD pattern overlay of PAZ·FFA·ACN-I simulated from SC-XRD (red), PAZ·FFA·ACN-II simulated from SC-XRD (blue), acetonitrile drops grinding preparation of PAZ·FFA·ACN-II (green), and after heating grinding preparation (maroon). The highlighted regions showed a significant difference in diffraction pattern.

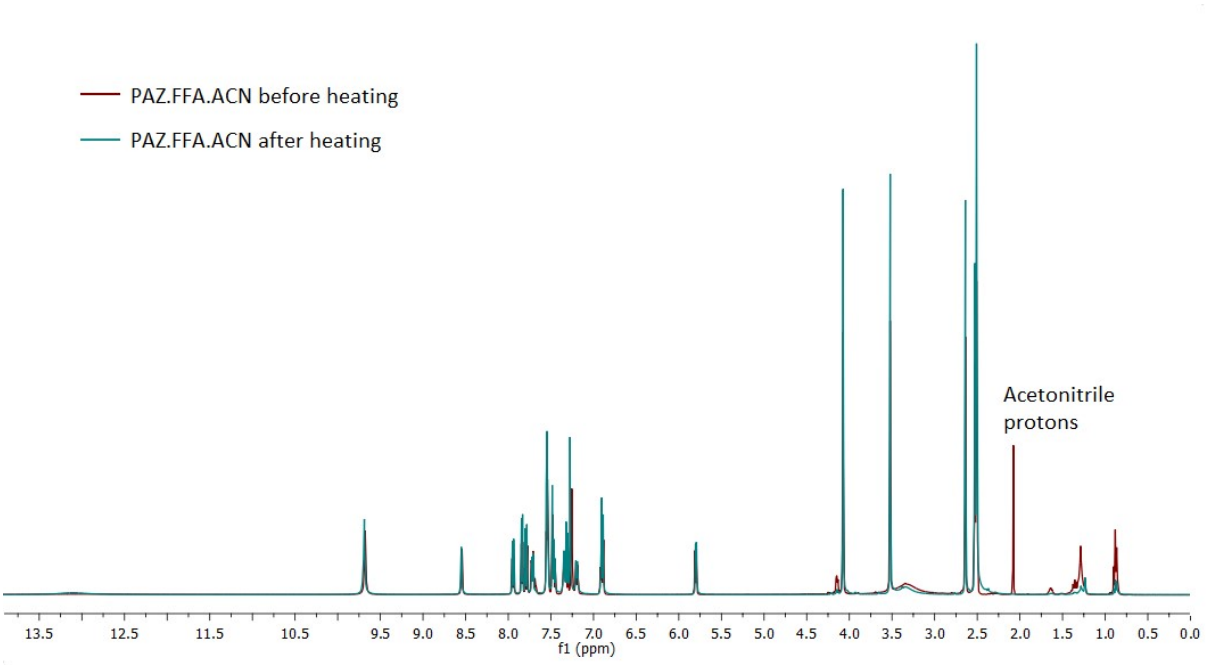

Fig. S11. ^{1}H NMR spectra of acetonitrile drops grinding preparation of PAZ·FFA·ACN sample before and after heating at 120 °C for one hour. Spectra were recorded at 400 MHz in DMSO-d_6 solvent.